Influence of Weld Process Parameters on Material Characterization of Friction Stir Welded Joints of Aluminium Alloy AA6061-T$_6$

H. S. Patil*

Department of Mechanical Engineering,
Pacific School of Engineering, Palsana, Surat, India
Email:hspatil12@rediffmail.com,hspatil28@gmail.com
*Corresponding author

S. N. Soman

Department of Metallurgy & Material Engineering,
Faculty of Engineering Technology, M. S. University of Baroda, India
Email:somansn@yahoo.com

Abstract: Friction stir welding, a solid state innovative joining technique, is widely being used to join aluminium alloys for aerospace, marine automotive and many other applications of commercial importance. FSW trials were carried out using a vertical machining centre (VMC) on AA6061 alloy. The main objective of the present work was to evaluate the weld processing parameter of friction stir weld (FSW) process for AA6061-T6 alloy and to determine the properties of the obtained joints with respect of welding speed. Experiments have been conducted by varying the welding speed of 55-70 mm/min and the rotating speed was fixed at 1700 rpm. Tensile properties, microstructure, microhardness, fractography, and corrosion resistance of FSW joints were investigated in this study. The result showed that there was a variation of grain size in each weld zone which depends upon the material and process parameters of FSW in the joint itself. The coarsest grain size was observed in heat affected zone (HAZ), followed by the thermomechanically affected zone (TMAZ) and the nugget zone (NZ). The maximum tensile strength of 184 MPa and highest joint efficiency of 49.32% were obtained on the joint fabricated at 55mm/min of welding speed.

Reference: Patil, H. S., and Soman, S. N., "Influence of weld process parameters on material characterization of friction stir welded joints of aluminium alloy AA6061-T6", Int J of Advanced Design and Manufacturing Technology, Vol. 6/ No. 4, 2013, pp. 9-15.

Biographical notes: H. S. Patil is perusing PhD in Mechanical Engineering from Veer Narmad South Gujarat University, Surat, Gujarat, India. His current research interest includes design and manufacturing. **S. N. Soman** received his PhD in metallurgy from IIT Bombay. His current research interest includes welding, corrosion.

1   INTRODUCTION

AA6061-T6 alloys are high-strength aluminium (Al), magnesium (Mg), and silicon (Si) alloys that contain manganese to increase their ductility and toughness. Alloys of this class are readily weldable, but they suffer from severe softening in the heat-affected zone (HAZ) because of dissolution of Mg2Si precipitates during the thermal cycle. It is therefore appropriate to overcome or minimize the HAZ softening with respect to the fusion welding, in order to improve mechanical properties of weldment [1]. In addition, the poor solidification microstructure and porosity in the fusion zone should also be overcome. Compared to many of the fusion welding processes that are routinely used for joining structural alloys, friction stir welding (FSW) is an emerging solid state joining process in which the material that is being welded does not melt and recast.

Friction stir welding was invented at The Welding Institute (TWI), UK in 1991. This is a solid-state process based on plastic deformation. Friction stir welding is a continuous, hot shear, autogenous process involving non-consumable rotating tool of the harder material than the substrate. Defect-free welds with good mechanical properties have been made in a variety of aluminium alloys, even those previously thought to be not weldable. When alloys are friction stir welded, phase transformations that occur during the cool down of the weld are of a solid-state type. Due to the absence of parent metal melting, the new FSW process is observed to offer several advantages over fusion welding [2-4].
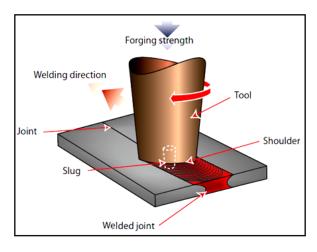

Fig. 1   Principle of FSW process

In this process a special slug rotating at high speed penetrates to the centre of the two pieces to be joined. The heat generated through friction makes the material soften into a paste-like phase (plasticize) [5]. Plastic deformation causes the edges of the material to mix together and fuse, as the term "friction stir weld" signifies. The presence of a retaining wall exerts sufficient force to prevent the semi-molten mixture from flowing out of the joint area. This creates a press forging effect behind the material which has been softened and mixed. Welding by plastic deformation is the technique of choice when maintaining the original properties of the metal is all-important. Since the tool heats the material to a paste-like consistency, and not liquid state, the properties of the material are not degraded to the same degree as they are when fusion occurs.

Fig. 1 explains the working principle of FSW process. FSW offers a quality advantage that leads the welds strength and ductility either identical or better than that of the base metal alloy [6]. Tensile strength of FSW is directly proportional to the welding speed [7]. The tensile strength of the friction stir welded is affected by the tool pin profile. The grain structure within the friction stir processing is fine and equiaxed compared to TMAZ [8]. Optimization of FSW parameters in different conditions of base material and the microstructures of the as-welded condition are compared with the post-weld heat treated microstructures welded in annealed and T6 condition [9]. FSW joints usually consist of four different regions as shown in fig.2. They are: A-Weld nugget (WN), B-Thermo-mechanically affected zone (TMAZ), C-Heat affected zone (HAZ), and D-Parent material (PM). The formation of the above regions is affected by the material flow behaviour under the action of rotating non-consumable tool [10]. However, the material flow behaviour is predominantly influenced by the FSW tool profiles and dimensions, and FSW process parameters [11], [12].
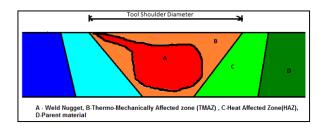

Fig. 2   Different regions of FSW joint

The weld zones are more susceptible to corrosion than the parent metal [13-18]. Generally, it has been found that Friction stir (FS) welds of aluminium alloys such as 2219, 2195, 2024, 7075 and 6013 did not exhibit enhanced corrosion of the weld zones. FSW of aluminium alloys exhibit intergranular corrosion mainly located along the nugget's heat-affected zone (HAZ) and enhanced by the coarsening of the grain

boundary precipitates. Coarse precipitates and wide precipitate-free zones promoted by the thermal excursion during the welding are correlated with the intergranular corrosion. The effect of FSW parameters on corrosion behaviour of friction stir welded joints was reported by many workers [16], [18]. The effect of processing parameters such as rotation speed and traverse speed on corrosion behaviour of friction stir processed high strength precipitation-hardenable AA2219-T87 alloy was investigated by Surekha et al. [18].

The available literature focuses on the effect of tool profiles and tool shoulder diameter on FSW zone formation. Hence, in this investigation an attempt has been made to understand the effect of welding speed on material characterization of AA6061 in terms of mechanical properties, metallurgical behaviour and corrosion analysis. This paper presents the effect of different welding speeds on the weld characteristics of AA6061-T6 fabricated by a hexagonal tool pin profile. The weld characteristic includes UTS, YS and %

elongation, microhardness, fractography, microstructure, and corrosion of AA6061-T6 joints.

2   EXPERIMENTAL DETAILS AND PROCESS CONDITIONS

The rolled plates of 5 mm thickness, AA6061 aluminium alloy were cut into the required sizes (300×150 mm) by power hacksaw cutting and grinding. The chemical composition and mechanical properties of the parent metal are presented in Table1. Square butt joint configuration was prepared to fabricate FSW joints. The initial joint configuration was obtained by securing the plates in position using mechanical clamps. The direction of welding was normal to the rolling direction. Single pass welding procedure was adopted to fabricate the joints. In present work hexagonal tool pin profile was used for the welds, made of cold work die steel (Figure3). The machine used for the production of the joints was vertical machining centre.

Table 1   Chemical composition and mechanical properties AA6061-T6

Chemical Composition								
Element	Si	Fe	Cu	Mn	Mg	Cr	Zn	Ti
Required	0.4-8	0.7	0.15-0.4	0.15	0.8-1.2	0.04-0.35	0.25	0.15
Contents	0.62	0.45	0.2	0.18	1.05	0.09	0.03	0.07

Mechanical Properties							
Tensile Strenght (MPa)		Yield Strenght (MPa)		Elongation (%)		Hardness (HV)	
Min	Max	Min	Max	Min	Max		
300	--	241	--	6	--	95	
328.57	335.71	282	296	11	11.8	98	

Fig. 3   Geometry of the hexagonal tool pin profile used in the present study

The welding parameters and tool dimensions are presented in Table 2. The welded joints were sliced using pantograph machine to the required dimensions to prepare tensile specimens. American Society for Testing of Materials (ASTM E8-04) guidelines were followed for preparing the test specimens. Tensile test

was carried out in 400 KN capacity mechanical controlled universal testing machine.

Table 2   Welding conditions employed to join AA6061 plates

Weld Process Parameter	Values
Rotational Speed (rpm)	17000
Welding Speed (mm/min)	55, 60, 65, 70
Tool Depth (mm)	4.6
Tool shoulder diameter(mm)	18
Pin diameter(mm)	6
Downward Force(KN)	11

All welded samples were visually inspected in order to verify the presence of possible macroscopic external defects, such as surface irregularities, excessive flash, and surface-open tunnels. By using Radiographic unit, X-Ray radiographic inspection was carried out on FSW samples. In radiographic test 6Ci & Ir192 used as

radioactive source. The film used was Agfa D-4 and the radiographs indicated defect-free weld as well as weld with defects like insufficient fusion and cavity. Mechanical properties of the test welds were assessed by means of tensile tests and the ultimate tensile stress (UTS) yield strength (YS) and % elongation were measured in the tensile test.

Microindentation hardness test as per ASTM E-384:2006 has been used to measure the Vickers hardness of FSW joints. The Vickers microhardness indenter is made of diamond in the form of a square-base pyramid. The test load applied was 100 gram and the dwell time was 15 seconds. The indentations were made at midsection of the thickness of the plates across the joint. The tensile fractured surfaces were analyzed by using scanning electron microscopy.

Metallographic specimens were cut mechanically from the welds, embedded in resin and mechanically ground and polished using abrasive disks and cloths with water suspension of diamond particles. The chemical etchant was the Keller's reagent. The microstructures were observed on optical microscope.

Potentiodynamic polarization tests were used to study the pitting corrosion behaviour of AA6061 alloys. In the tests, cell current readings were taken during a short, slow sweep of the potential. The sweep was taken in the range of 0.5V to 1V. The potentiodynamic scan was performed at scan rate of 0.5mV/sec.

3   RESULTS AND DISCUSSION

3.1. Mechanical Properties

The mechanical and metallurgical behaviour of AA6061 was studied in this research. Transverse tensile properties of FSW joints such as yield strength, tensile strength, percentage of elongation and joint efficiency on transverse tensile specimens are presented in figure 5. The strength and ductility in the as-welded condition are lower than those of the parent metal in T_6 condition.

The heat input in the weld area is affected by welding conditions like welding speed and rotation rate. With constant rotational speed of 1700 rpm (Figure 4) and constant downward pressure of 11KN, higher welding speed resulted in lower heat input per unit length of the weld, causing lack of stir in the friction stir processing zone yielded poor tensile properties. Lower welding speed resulted in higher temperature and slower cooling rate in the weld zone causing grain growth and precipitates. Most of the joints fractured at the retreating side due to variation in temperature distribution and flow of the material in the weld zone with corresponding hardness distribution and strained region. It can be observed that the flow of the parent material on the advancing side and the retreating side are different. The

material on the retreating side never enters into the rotational zone, while the material on the advancing side form the fluidized bed near the pin and rotates around it.
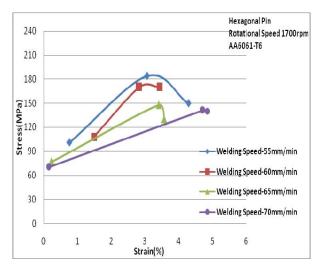

Fig. 4   Stress-Strain curves for AA6061-T6 of hexagonal pin

During friction stir welding the heat is assumed to be produced mainly through the friction between the tool shoulder and the plate surface. Therefore, the heat is no longer concentrated to a narrow line, but rather generated throughout a broad band having the width of the tool shoulder. The tangential velocity of the rotating tool shoulder surface is high at the periphery hence; the strongest temperature gradients are not expected to be in the weld line but at the edges of the shoulder resulted in thermal softening.

The location of the soft band is at the retreating side where precipitates over aging contribute failure at this region. Hence, the welding speed must be optimized to get FSP region with fine precipitates uniformly distributed throughout the matrix. Of the four different welding speeds (55-70 mm/min), the joints fabricated at the welding speed of 55 mm/min exhibited superior tensile properties of 184 N/mm^2 UTS and joint efficiency of 49.32 %. The combined effect of higher number of pulsating stirring action during metal flow and an optimum welding speed may be the reason for superior tensile properties of the joint fabricated at the welding speed of 55 mm/min using hexagonal pin profiled tool (Figures 4-5).

In FSW, microhardness reflects the state of precipitates within the WAZ as well since the alloy composition is fixed, changes in microhardness must result primarily from changes in precipitates and grain size. Microhardness plots for welds performed with different welding speed can be seen for the AA6061 alloy in figure 6. The results show that the friction stir processed area has an equivalent Vickers hardness value with respect to the parent material.
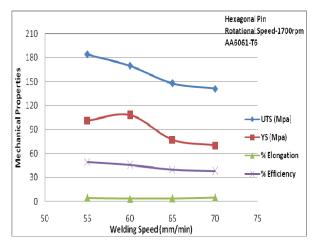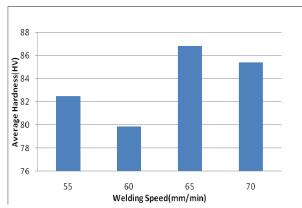
Fig. 5 Effect of welding speed on mechanical properties of AA6061-T$_6$,

Fig. 6 Effect of welding speed on microhardness of AA6061-T$_6$,

3.2. Metallographic Analysis

Based on optical micro-structural characterization of grains and precipitates, three distinct zones have been identified i.e. weld nugget zone, thermo-mechanically affected zone (TMAZ) and heat affected zone (HAZ). Microstructural details of the parent metals (PM) and the similar joint are presented in figures 7-9. The parent material revealed grains of unequal sizes and was seen distributed in the matrix with the grains tending to be rather elongated. The frictional heat provided by rubbing of the tool shoulder and mechanical stirring of the material by the tool nib, the adiabatic heat arising from the deformation induced dynamic recrystallization and the result shows transition of aluminium from the parent material to the FSW zone with a clean decrease in grain size.

3.3. Fractography Analysis

Examination of the tensile fracture surfaces of AA6061 was done at both low and high magnifications in order to identify the fracture mechanisms. The SEM observations of the fracture surfaces of the tensile tested specimens revealed the best bonding characteristics of the FSW joints. The fracture surface appears populated of very fine dimples revealing a very ductile behaviour of the material before failure as shown in figure 10.
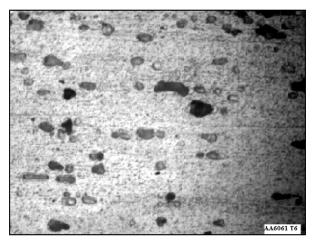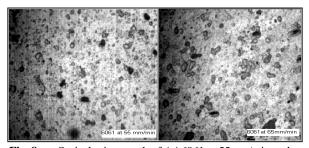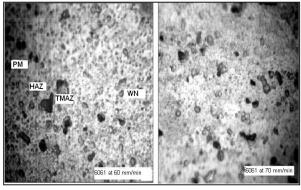

Fig. 7 Optical micrograph of parent metal AA6061

Fig. 8 Optical micrograph of AA6061 at 55mm/min and at 65mm/min

Fig. 9 Optical micrograph of AA6061 at 60mm/min and at 70mm/min

3.4. Corrosion Behaviour

The potentiostatic polarization curves for the base alloy and FSW samples in 3.5%NaCl at room temperature are given in figures 11-12. It is shown that the corrosion behavior of parent alloy significantly varies from that of welded joints.
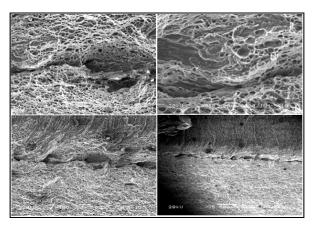
Fig. 10   SEM images of tensile fracture surface of AA6061 at 65mm/min

Table 3   Result analysis of corrosion test

Material of FSW Joint	Welding Speed(mm/mim)	I_{corr} (µA/cm^2)	E_{corr}(mV)	Corrosion Rate (mpy)
$6061T_6$-$6061T_6$	55	471 nA	-841	215.3 e^{-3}
$6061T_6$-$6061T_6$	60	202.0 nA	-789	92.23 e^{-3}
$6061T_6$-$6061T_6$	65	3.34	-1.35V	1.526
$6061T_6$-$6061T_6$	70	1.35	-1200	617.7 e^{-3}
PM AA6061T$_6$	--	1.82	-1160	832.1 e^{-3}

From table 3 it is observed that the pitting potentials of corrosion tested samples at various process parameters clearly indicated a greater corrosion resistance of weld metal than base metal. This is attributed to the precipitates present in the alloy promote matrix dissolution through selective dissolution of aluminium from the particle. These precipitate deposits are highly cathodic compared to the metallic matrix, which initiates pitting at the surrounding matrix and also enhances pit growth.
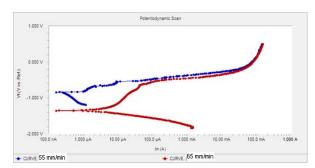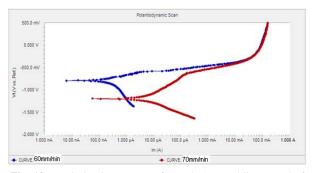

Fig. 11   Polarization curves of AA6061 at welding speed of 55-65mm/min

During FSW process only coarser precipitates could nucleate and grow but not finer ones. This aids in formation of passive film, which remained more intact on surface of the sample. It is also found that in AA6061 at 65 mm/min, the corrosion resistance is very poor. The poor pitting corrosion resistance of weld joint is due to difference in pitting potentials across the

weld region or stir nugget because of inhomogeneity of microstructures in those regions. All FSW samples show passivation after longer exposure to corrosion media. AA6061 at 65 mm/min has highest active potential (-1.35V). The active E_{corr} increased with increasing the weld speed.

Fig. 12   Polarization curves of AA6061 at welding speed of 60-70mm/min

4   CONCLUSION

The mechanical and metallurgical behaviour of AA6061 was studied in this paper. The joints were produced with different welding speed from 55 to 70 mm/min and maintaining constant rotational speed of 1700 rpm. Downward force was observed to be constant as the welding speed for all the produced joints increases. The tensile strength of the FSW joint is lower than that of the parent metal. With the increase in

welding speed above critical value, tensile strength and % elongation decreases due to low heat input at constant downward pressure and tool rotational speed. Out of four different welding speeds (55-70 mm/min), the joints fabricated at a welding speed of 55 mm/min exhibited superior tensile properties of 184 N/mm^2 UTS and joint efficiency of 49.32%. Microstructural changes induced by the friction stir welding process were clearly identified in this study. Friction stir welding of AA6060-T$_6$ resulted in a dynamically recrystalized zone, TMAZ and HAZ. A softened region has clearly occurred in the friction stir welded joints due to dissolution of strengthening precipitates. The fracture surface appears populated of very fine dimples revealing a very ductile behaviour of the material before failure. Corrosion rate is increased by increasing the welding speed of FSW tool.

REFERENCES

[1] Elangovan, K., Balasubramanian, V., and Babu, S., "Predicting tensile strength of friction stir welded AA6061 aluminium alloy joints by a mathematical model", Materials and Design, Vol. 30, 2009, pp. 188-193.

[2] Thomas, W. M, et al., "Friction stir welding. International Patent Application No. PCT/GB92/02203 and GB Patent Application No. 9125978.8", US Patent No. 5, 460,317, 1991.

[3] Threadgill, P. L., "Friction stir welding - The state of the art, Bulletin 678", TWI, UK, 1999.

[4] Peel, M., Steuwer, A., Preuss, M., and Withers, P. J., "Microstructure, mechanical properties and residual stresses as a function of welding speed in AA5083 friction stir welds", Acta Mater, Vol. 51, 2003, pp. 4791-801.

[5] Mishra, R. S., and Ma, Z. Y., "Friction stir welding and processing", Materials Science and Engineering: R: Reports, Vol. 50, 2005, pp. 1-78.

[6] Naiyi, L., Tsung-Yu Pan, Ronald, P., Cooper, D., Houston, Q., Zhili, F., and Michael, L., "Santella, FSW of magnesium alloy AM60", 19 Magnesium Technology 2004 Edited by Alan A. Luo TMS (The Minerals, Metals & Materials Society), 2004.

[7] Adamowski, J., and Szkodo, M., "Friction Stir Welds (FSW) of aluminum alloy AW6082-T6 GSE", Ansaldo Energia, Via Lorenzi 8, 16100 Genoa, Italy Vol. 20, No. 1-2 , 2007.

[8] Palanivel, R., Koshy Mathews, P., and Murugan, N., "Influences of tool pin profiles on the mechanical and metallurgical properties of FSW of dissimilar alloys" International Journal of Engineering Science and Technology, Vol. 2, No.6, 2010, pp. 2109-2115.

[9] Indira Rani, M., Marpu, R. N., and Kumar, A. C. S., " A study of process parameters of friction stir welded AA 6061 aluminum alloy in O and T6 conditions" ARPN Journal of Engineering and Applied Sciences, Vol. 6, No. 2, February 2011.

[10] Murr, L. E., Flores, R. D., Flores, O. V., McClure, J. C., Liu, G., and Brown, D., "Friction-stir welding: microstructural characterization", Mater Res Innov, Vol. 1, No. 4, 1998, pp. 211-23.

[11] Huijie, L., Fujii, H., Maeda, M., and Nogi, K., "Heterogeneity of mechanical properties of friction stir welded joints of 1050-H 24 aluminium alloy", Journal Mater Sci. Lett., Vol. 22, 2003, pp. 441-4.

[12] Liu, H. J., Fuji, H., Maeda, M., and Nogi, K., "Mechanical properties of friction stir welded joints of 1050-H 24 aluminium alloy", Sci. Technol. Weld Join, Vol. 8, 2003, pp. 450-4.

[13] Paglia, C. S., Jata, K.V., and Buchheit, R.G., "A cast 7050 friction stir weld with scandium: microstructure, corrosion and environmental assisted cracking", Material Science Engineering- A, Vol. 424, 2006, pp. 196-204.

[14] Fonda, R. W., Pao, P. S., Jones, H. N., Feng, C. R., Connolly, B. J., and Davenport, A. J., "Microstructure, mechanical properties, and corrosion of friction stir welded Al 5456", Material Science Engineering- A, Vol. 519, 2009, pp. 1-8.

[15] Wadeson, D. A., Zhou, X., Thompson, G. E., Skeldon, P., Djapic Oosterkamp, L., and Scamans, G., "Corrosion behaviour of friction stir welded AA7108 T79 aluminium alloy", Corrosion Science, Vol. 48, 2006, pp. 887-897.

[16] Jariyaboon, M., Davenport, A. J., Ambat, R., Connolly, B. J., Williams, S. W., and Price, D. A., "The effect of welding parameters on the corrosion behaviour of friction stir welded AA2024–T351", Corrosion Science, Vol. 49, 2007, pp. 877-909.

[17] Pao, P. S., Gill, S. J., Feng, C. R., and Sankaran, K. K., "Corrosion-fatigue crack growth in friction stir welded Al 7075", Scripta Materiala, Vol. 45, 2001, pp. 605-612.

[18] Surekha, K., Murty, B. S., and Prasad Rao, K., "Effect of processing parameters on the corrosion behaviour of friction stir processed AA2219 aluminium alloy", Solid State Sciences, Vol. 11, 2009, pp. 907-917.